CSIRO PUBLISHING
www.publish.csiro.au/journals/ajar *Australian Journal of Agricultural Research*, 2008, **59**, 112–126

Quality and potential utility of ENSO-based forecasts of spring rainfall and wheat yield in south-eastern Australia

M. R. Anwar[A,E], *D. Rodriguez*[B], *D. L. Liu*[C], *S. Power*[D], *and G. J. O'Leary*[A]

[A]Primary Industries Research Victoria, 110 Natimuk Rd, Horsham, Vic. 3400, Australia.
[B]Agricultural Production Research Unit (APSRU), Queensland Department of Primary Industries & Fisheries, PO Box 102, Toowoomba, Qld 4350, Australia.
[C]E.H. Graham Centre for Agricultural Innovation (NSW Department of Primary Industries and Charles Sturt University), Wagga Wagga Agricultural Institute, PMB Wagga Wagga, NSW 2650, Australia.
[D]Bureau of Meteorology, GPO Box 1289, Melbourne, Vic. 3001, Australia.
[E]Corresponding author. Email: muhuddin.anwar@dpi.vic.gov.au

Abstract. Reliable seasonal climate forecasts are needed to aid tactical crop management decisions in south-eastern Australia (SEA). In this study we assessed the quality of two existing forecasting systems, i.e. the five phases of the Southern Oscillation Index (SOI) and a three phase Pacific Ocean sea-surface temperatures (SSTs), to predict spring rainfall (i.e. rainfall from 1 September to 31 November), and simulated wheat yield. The quality of the forecasts was evaluated by analysing four attributes of their performance: their reliability, the relative degree of shift and dispersion of the distributions, and measure of forecast consistency or skill. Available data included 117 years of spring rainfall and 104 years of grain yield simulated using the Agricultural Production Systems Simulator (APSIM) model, from four locations in SEA. Average values of spring rainfall were 102–174 mm with a coefficient of variation (CV) of 47%. Average simulated wheat yields were highest (5609 kg/ha) in Albury (New South Wales) and lowest (1668 kg/ha) in Birchip (Victoria). The average CV for simulated grain yields was 36%. Griffith (NSW) had the highest yield variability (CV = 50%). Some of this year-to-year variation was related to the El Niño Southern Oscillation (ENSO). Spring rainfall and simulated wheat yields showed a clear association with the SOI and SST phases at the end of July. Important variations in shift and dispersion in spring rainfall and simulated wheat yields were observed across the studied locations. The forecasts showed good reliability, indicating that both forecasting systems could be used with confidence to forecast spring rainfall or wheat yield as early as the end of July. The consistency of the forecast of spring rainfall and simulated wheat yield was 60–83%. We concluded that adequate forecasts of spring rainfall and grain yield could be produced at the end of July, using both the SOI and SST phase systems. These results are discussed in relation to the potential benefit of making tactical top-dress applications of nitrogen fertilisers during early August.

Additional keywords: APSIM, simulated yield, absolute median difference, dispersion, reliability, skill.

Introduction

Crop production in south-eastern Australia (SEA) is highly sensitive to present inter-annual climatic variability (Power *et al*. 1999; Potgieter *et al*. 2002). Probabilistic seasonal climate forecasts (SCF), capable of predicting some of this variability (Rimmington and Nicholls 1993; Hammer *et al*. 1996), are widely available to decision makers. However, even when widely used in Queensland and northern New South Wales (Meinke and Hochman 2000; Stephens *et al*. 2000; Hayman and Fawcett 2004), their value for in-season decision making in SEA remains uncertain. The Southern Oscillation Index (SOI) phase forecasting system has been shown to have economic value for farmers in southern Queensland (Hammer *et al*. 1996). Useful signals from El Niño Southern Oscillation (ENSO) have also been reported for the south-eastern grain belt (Power *et al*. 1998), and correlations between the SOI and May–October rainfall have been observed for some regions of southern Australia (Hayman and Fawcett 2004; www.cvap.gov.au).

Probabilistic rainfall forecasts for the months of August, September, and October could be used to assist farmers make better tactical changes in in-crop management such us top-dressing nitrogen (Lythgoe *et al*. 2004). In the SEA region, wheat is usually sown between May and July with no or small amounts of nitrogen fertilisers (Angus 2001), generally on dry soils, and irrespective of expected seasonal conditions. In addition, crops mostly rely on seasonal rainfall during the spring months (Sadras *et al*. 2002) as stored soil water is usually minimal due to shallow soils or the presence of subsoil constraints (Sadras *et al*. 2003; Rodriguez *et al*. 2006). Uncertainty on seasonal rainfall makes farmers avoid expensive and risky practices such as the use of nitrogen fertilisers at sowing, thereby limiting yields during the best seasons (Lythgoe *et al*. 2004). The availability of reliable forecasts during late autumn can be important for farmers to adjust crop nitrogen nutrition to expected seasonal conditions.

In this paper we aim to: (*i*) quantify the predictive capacity of the SOI 5-phase system (Stone and Auliciems 1992 in Stone

 10.1071/AR07061 0004-9409/08/020112

et al. 1996), and the Pacific Ocean SST phases (Drosdowsky 2002) at the end of July, a time of the year when farmers decide whether or not to top dress crops with extra nitrogen; and (*ii*) to test if the predictive capacity of these forecasting systems can be improved by predicting an integrative variable, i.e. simulated wheat yields, instead of forecasting rainfall. We also explore the conditions required for the effective use of ENSO-related wheat yield and seasonal climate forecasts, and investigate forecast quality (Potgieter *et al*. 2003) and the association of spring rainfall and wheat yields with SOI and SST phases.

Materials and methods

Site and climate data

Historical climate data (1 January 1900–31 December 2003) from four locations within major wheat-growing areas of SEA, i.e. Birchip (35.98°S, 142.92°E) and Dooen (36.67°S, 142.30°E) in Victoria, and Albury (36.07°S, 146.96°E) and Griffith (34.25°S, 146.07°E) in New South Wales, were obtained from the SILO website (www.bom.gov.au/silo/, 2005). Major differences in the production systems across the studied locations included differences in soil properties, crop cultivars, planting dates, plant densities, nitrogen practices, and climatic conditions (Tables 1 and 2).

Seasonal climate forecasts

Several medium-term climate forecasting systems are available (Stone *et al*. 1996; Drosdowsky 2002) that provide seasonal climate forecasts over the few subsequent months. However, for the effective application of seasonal climate forecasting, targetted and relevant information capable of influencing decisions is needed (Hammer 2000). In cropping, relevant and targetted information usually relates to the effect of a particular decision on the yield or profitability of the cropping enterprise. In this work, we used a cropping systems simulator to produce information that is highly relevant to the decision maker, i.e. wheat yields, and tested the capacity of the 5-phase SOI system (Stone and Auliciems 1992) and a 3-phase Pacific Ocean SSTs system (Drosdowsky 2002) to forecast spring rainfall and wheat yield. We analysed the spring rainfall, as rainfall between 1 September and 31 November. Analogue years with the same SOI phase over the June–July months were obtained from the long-paddock website (www.longpaddock.qld.gov.au/), and years in history with the same Pacific Ocean SST phase in July were obtained from the website of the Bureau of Meteorology (www.bom.gov.au) (Table 3).

Simulation of wheat yields

We used the Agricultural Production Systems Simulator (APSIM-wheat) model (McCown *et al*. 1996; Keating *et al*. 2003) Version 3.6 to simulate wheat yields. This model simulates the development, growth, and final yield of several crops under prescribed management, as well as the changes in soil water and soil nitrogen supply during the cropping season (Asseng *et al*. 1998; Rodriguez and Nuttal 2003; Sadras *et al*. 2003). APSIM-wheat has been previously used to identify crop management

Table 1. Soil type, plant-available water capacity (PAWC), initial available water (AW), rooting depth (depending on subsoil salinity), soil nitrogen and C : N ratio in the previous crop residues used for wheat crop simulation with APSIM, and annual and seasonal (April–October) rainfall for 4 regions across south-eastern Australia

Location	Soil	PAWC (mm)	AW (mm)	Rooting depth (m)	NO_3-N (kg/ha)	C : N in residue	Annual rain (mm)	Seasonal rain (mm)
				Victoria				
(Southern Mallee) Birchip	Red-coloured Calcarosol	94	42	0.6–0.8	17	80	371	253
(Wimmera) Dooen	Grey cracking clay	179	47	1–1.2	35	24	420	300
				New South Wales				
Albury	Red Padzolic	124	25	1.5	60	50	664	446
Griffith	Red brown earth	146	15	1.2–1.5	45	50	400	248

Table 2. Common agronomic practices for rainfed wheat production and the basic assumptions for wheat crop simulation with APSIM

Location	Cultivar	Plants/m^2	Sowing	Nitrogen and tillage management
			Victoria	
(Southern Mallee) Birchip	Frame	140	7 May–15 July	Pre-drilled: 20 kg N/ha as urea. Sowing: 20 kg N/ha as urea. Residues burnt, and 2 cultivations before sowing
(Wimmera) Dooen	Frame	140	1 May–20 June	Pre-drilled: 54 kg N/ha as urea. Sowing: 20 kg N/ha as urea. Residues burnt, and 1–2 cultivations before sowing
			New South Wales	
Albury	Diamondbird	120	1 May–13 June	Sowing: 40 kg N/ha as (MAP) Monoammonium phosphate. Spring top-dressing: 60 kg N/ha as urea. Residues burnt, and 1–2 cultivations before sowing
Griffith	Diamondbird	80	21 April–14 June	Sowing: 50 kg N/ha as urea. Spring top-dressing: 40 kg N/ha as urea. Residues burnt, and 1–2 cultivations before sowing

Table 3. The analogue years for the 5-phase SOI system and the 3-phase SST system in June–July between 1900 and 2003
The SOI phases relate to trends in the SOI over the 2-month period. For SST phases, 'Cold Pacific' represents La Niña events, 'Warm Pacific' represents El Niño events and the remainder are Neutral in July

	Years
	SOI phase
Consistently negative (CN)	1905, 1911, 1914, 1919, 1940, 1941, 1946, 1972, 1977, 1982, 1987, 1992, 1993, 1994, 1997
Consistently positive (CP)	1900, 1901, 1909, 1910, 1917, 1920, 1921, 1924, 1931, 1934, 1938, 1945, 1950, 1952, 1955, 1956, 1964, 1968, 1973, 1975, 1981, 1986, 1989, 1996, 1998
Rapidly falling (RF)	1918, 1923, 1925, 1937, 1951, 1965, 1970, 1976
Rapidly rising (RR)	1903, 1906, 1912, 1916, 1926, 1928, 1933, 1936, 1939, 1943, 1947, 1948, 1949, 1954, 1960, 1963, 1974, 1979, 1984, 1985, 1988, 1995, 1999, 2003
Consistently near zero (NZ)	1902, 1904, 1907, 1908, 1913, 1915, 1922, 1927, 1929, 1930, 1932, 1935, 1942, 1944, 1953, 1957, 1958, 1959, 1961, 1962, 1966, 1967, 1969, 1971, 1978, 1980, 1983, 1990, 1991, 2000, 2001, 2002
	SST (Pacific Ocean) phases
Cold Pacific	1901, 1903, 1906, 1908, 1909, 1910, 1913, 1916, 1917, 1921, 1922, 1929, 1933, 1938, 1941, 1946, 1950, 1954, 1955, 1956, 1959, 1964, 1967, 1970, 1971, 1974, 1975, 1978, 1981, 1984, 1985, 1986, 1988, 1989, 1994, 1996, 1999, 2000
Neutral Pacific	1904, 1907, 1911, 1912, 1915, 1919, 1920, 1923, 1924, 1927, 1928, 1930, 1931, 1934, 1935, 1936, 1937, 1939, 1942, 1943, 1945, 1947, 1948, 1949, 1952, 1960, 1961, 1962, 1966, 1968, 1973, 1979, 1980, 1990, 1993, 2001
Warm Pacific	1900, 1902, 1905, 1914, 1918, 1925, 1926, 1932, 1940, 1944, 1951, 1953, 1957, 1958, 1963, 1965, 1969, 1972, 1976, 1977, 1982, 1983, 1987, 1991, 1992, 1995, 1997, 1998, 2002, 2003

strategies and quantify benefits from the adoption of seasonal climate forecasts to reduce risks in wheat cropping (Hammer *et al*. 1996; Lythgoe *et al*. 2004). The model APSIM-Wheat was parameterised with the modules SOILN2, SOILWAT2, and RESIDUE2. The phenology parameters were calibrated for the cv. Frame at Birchip and cv. Matong at Dooen. Values of soil water content at saturation (SAT) were calculated from values of bulk density (Dalgliesh and Foale 1998), and values of drainage upper limit (DUL) were measured in the field (Nuttall *et al*. 2003). Crop water lower limits (LL) were taken as soil water contents determined in the laboratory at −1500 kPa. Crop management practices were obtained from experienced agronomists for each of the regions (Tables 1 and 2), and starting conditions (soil water, soil N and residues) for each simulation were set on the 1 January of each simulated year. The agreement between observed and simulated results was evaluated by comparing the coefficient of determination and root mean square deviation (RMSD).

Associations of rainfall and yield with the climate phases

A contingency table was built to test whether effects (associations) were present between spring rainfall or simulated wheat yields, with SOI phases in June–July and/or with the Pacific Ocean SST phase in July. The statistical significance ($P < 0.05$) of such deviations was assessed by a χ^2 (Chi-square) test (Wilks 1995).

Forecast quality

A variety of forecast verification procedures exists, although they all usually involve measures of the relationship between a forecast and the corresponding observation of the predicand (Wilks 1995). In this work we have assessed the quality of two probabilistic forecasts by studying four attributes of their performance, their reliability, the relative degree of shift and dispersion of the distributions (Wilks 1995; Potgieter *et al*. 2003), and measure of forecast consistency.

Reliability

Forecast verification is the process of assessing the quality of a forecast. A deterministic forecast can be compared or verified, against a corresponding observation of what actually occurred, or a good estimate of the true outcome. By definition, probabilistic forecasts cannot be defined as correct or incorrect. However, probabilistic forecasts can be assessed as 'reliable' in the sense that when a forecaster says that there is a high probability of rain, it should rain more than when the forecaster says there is a low probability of rain. Reliability plots (Fig. 1) are used to

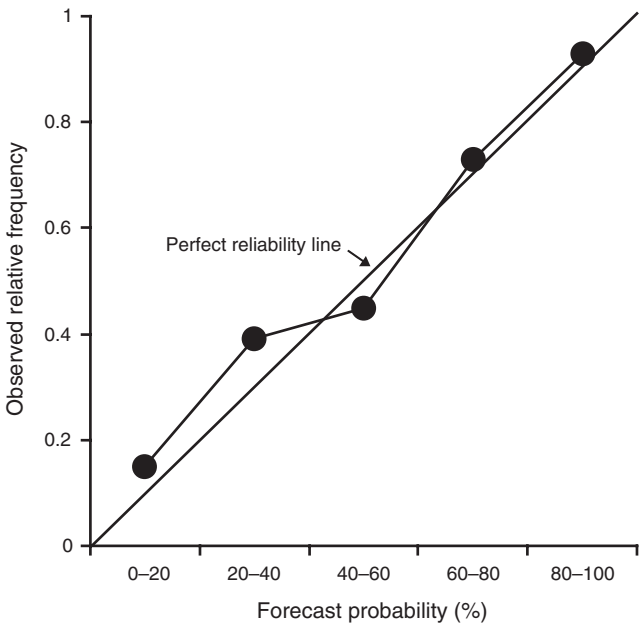

Fig. 1. The reliability diagram (Wilks 1995) graphically relates the observed relative frequency to each possible forecast probability.

indicate the reliability of a probabilistic forecast (Wilks 1995). The reliability plot summarises the information contained in the conditional distribution [P(O|f)] and describes how often an observation occurred given a particular forecast (Wilks 1995). Ideally,

$$P(O|f) = f \quad (1)$$

i.e. for the set of forecasts where a forecast probability value f was given to a particular observation, O, the forecast is considered perfectly reliable if the relative frequency of the observations equals the forecast probability (Wilks 1995). The reliability plot graphically relates the observed relative frequency (ORF) to each possible forecast probability f. The conditional distribution of a set of perfectly reliable forecasts will fall along the 1 : 1 line between ORF and f (Murphy and Winkler 1992). In the present work we have quantified the reliability of forecasts of spring rainfall and wheat yields at the end of July, using the method described in Potgieter *et al*. (2003).

In Fig. 2, we show how the observed climate up to 31 July was projected to create spring rainfall and simulated wheat yield data plumes, for each year between 1889 and 2005. Individual data plumes or trajectories associated with the prevailing SOI or SST phases, i.e. analogue years, were used to derive the respective forecast distributions for spring rainfall and simulated wheat yields (Table 3). Long-term medians were calculated using all available records (n), i.e. 117 years of climate records were used for spring rainfall, and 104 years of climate records to simulate the wheat yields. For each of the forecasted distributions, i.e. using the 5 SOI and the 3 SST phase systems, we then calculated the probability of exceeding the long-term median (f). The values of f were then grouped into quintiles i.e. 0–20%, 20–40%, 40–60%, 60–80%, and 80–100%, and compared against the observed relative frequency (ORF) of realised forecasts, i.e. with respect to the total number of issued forecasts. The degree of reliability was estimated from the slope through the origin in the reliability plot, i.e. ORF *v.* the f interval. The root mean square deviation (RMSD) was calculated to indicate the deviation of the ORF values around the 1 : 1 line, and the values of the slope (b) were classified into reliability classes, i.e. poor ($b \leq 0.5$ or $b \geq 1.5$), moderate ($0.5 < b \leq 0.75$ or $1.25 \leq b < 1.5$), and good ($0.75 < b < 1.25$) (Potgieter *et al*. 2003).

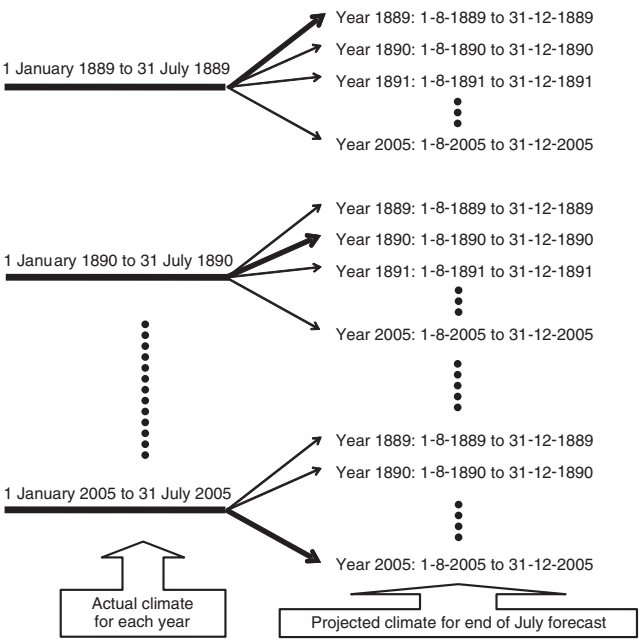

Fig. 2. Projected climate data trajectories using actual climate up to the time of forecast as proposed by Potgieter *et al*. (2003). Forecast distributions of projected climate were based on analogue years of June–July SOI phase. Dark black arrows indicate the actual climate.

Shift and dispersion

Kruskal–Wallis tests (KW) (Kruskal and Wallis 1952) were used to test the significance of shifts in median spring rainfall and simulated wheat yield, for each SOI/SST phase (forecasts), with respect to the rest of the years. Whenever significant differences were detected, a Kolmogorov–Smirnov test (KS) (Conover 1971) was used to test differences in the cumulative distributions between each of the individual phases and the rest of the years (Wilks 1995; Meinke *et al*. 1996). The absolute median difference (AMD) (Eqn 2) was used to quantify shifts in median values, and inter-quartile ratios (IQR) (Eqn 3) were used to quantify changes in dispersion in the distributions (Wilks 1995; Potgieter *et al*. 2003):

$$\text{Absolute median difference (AMD)} = |\overline{X}_R - \overline{X}_F| \quad (2)$$

where $\overline{X}_F$ and $\overline{X}_R$ are the sample medians of the forecasted and reference, i.e. rest of the years distributions;

$$\text{Inter-quartile ratio (IQR)} = \frac{(X_{75} - X_{25})\,F}{(X_{75} - X_{25})\,R} \quad (3)$$

where X_p indicates the percentile value (75% or 25%) for the forecasted and reference distributions, respectively. Values of the IQR higher (smaller) than 1 indicate a higher (smaller) dispersion (spread) in the forecasted values with respect to the reference distribution.

Forecast consistency

To independently verify the hindcast skill of the forecasting systems, a cross-validation technique was applied to spring rainfall and simulated yields. Cross-validation was used to ensure that the verification of the statistical prediction scheme is based on independent data. This is achieved by excluding some years when the statistical scheme is developed and then assessing the consistency of the statistical scheme developed in predicting the rainfall (or crop yield) in the years excluded (Wilks 1995). The methodology results in a measure of consistency expressed as 'percent consistent', i.e. the number of consistent forecasts for a category (e.g. above median), divided by the total number of forecasts made for that category (www.bom.gov.au). Experience shows that people have difficulty in understanding probabilistic forecasts. Some people initially interpret the information in a categorical sense, e.g. by assuming that the tercile with the highest probability is actually being forecasted categorically, ignoring the other two terciles even when all three tercile probabilities are non-zero. The use of the term 'Percent Correct' (Wilks 1995) in communications with end users can actually mislead and encourage users to erroneously regard the probabilistic forecasts as categorical forecasts. To avoid this, we follow the alternative term Percent

'Consistent' (S. Power, D. Solofa, W. Young, S. Williams, D. Jones, D. McClintock, J. Pahalad, unpublished data).

Results

Wheat simulations

Comparison of simulated and observed wheat yields for experimental data from the locations under study is shown in Fig. 3. The crop model was able to explain 74% of the observed variability in grain yields with a RMSD of 640 kg/ha. Given this adequate level of predictability, we applied the APSIM-wheat model to create long-term time series (1900 to 2003) of simulated yields of wheat based on common agronomic practices (Tables 1 and 2) at each of the studied locations. The long-term median simulated wheat yield ranged from 1826 to 5950 kg/ha across the locations (Table 4 and Fig. 7). The coefficient of variation (CV) of simulated wheat yield was 36% at Birchip, 37% at Dooen, 21% at Albury, and 50% at Griffith (Table 4). The highest value was obtained at Albury, NSW (5950 kg/ha), while the lowest was obtained at Birchip, Vic. (1826 kg/ha). As expected, the locations with higher rainfall usually produced higher grain yields (Table 4). The simulated time series of yield

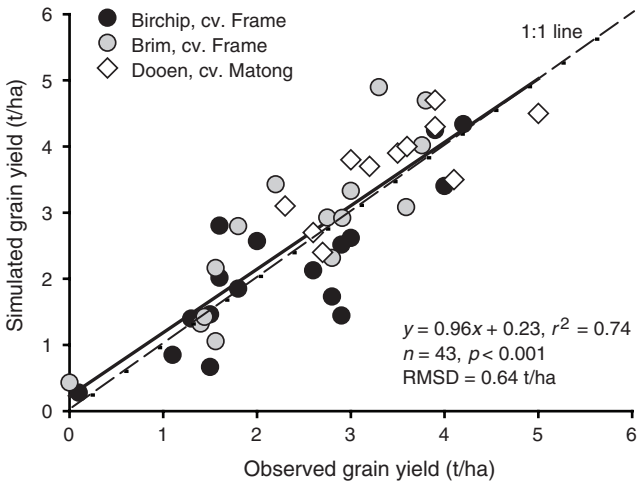

Fig. 3. Comparison of simulated and observed wheat yields at Birchip, Brim, and Dooen. Farm wheat yield data were used from 1983 to 2002 at Birchip and Brim, using cv. Frame, and from 1988 to 2001 at Dooen, using cv. Matong. Simulations were conducted with APSIM Version 3.6.

Table 4. Descriptive statistics for simulated wheat yields and climate variables at each of the studied locations

The numbers in parentheses next to the minimum and maximum indicate the year in which the extreme occurred, as well as the corresponding SOI/SSTs phases in June–July. CV%, Coefficient of variation; CN, consistently negative; CP, consistently positive; RF, rapidly falling; RR, rapidly rising; NZ, consistently near zero; C, Cold Pacific SSTs; N, Neutral Pacific SSTs; W, Warm Pacific SSTs

Statistic	Birchip	Dooen	Albury	Griffith
		Yield (kg/ha)		
Minimum	111 (1982, CN, W)	254 (1982, CN, W)	1708 (1914, CN, W)	199 (1902, NZ, W)
33rd percentile	1543	2579	5491	1876
Median	1826	2945	5950	2578
Average	1668	2708	5604	2679
66th percentile	2016	3304	6247	3280
Maximum	2658(1984, RR, C)	4138(1974, RR, C)	7197 (1986, CP, C)	5931 (1974, RR, C)
CV (%)	36	37	21	50
		Spring rainfall (mm)		
Minimum	9 (1982, CN, W)	16 (1967, NZ, C)	41 (1938, CP, C)	22 (1957, NZ, W)
33rd percentile	72	89	143	70
Median	97	108	172	94
Average	104	115	174	102
66th percentile	124	133	204	130
Maximum	266 (1975, CP, C)	283 (1975, CP, C)	451 (1992, CN, W)	233 (1916, RR, C)
CV (%)	48	46	44	50
		Annual rainfall (mm)		
Minimum	111 (1982, CN, W)	190 (1982, CN, W)	314 (1967, NZ, C)	166 (1902, NZ, W)
33rd percentile	330	373	580	342
Median	372	416	661	393
Average	371	416	664	399
66th percentile	421	456	741	446
Maximum	729 (1973, CP, N)	810 (1973, CP, N)	1138 (1939, RR, N)	720 (1974, RR, C)
CV (%)	28	25	26	30
		Seasonal rainfall (mm)		
Minimum	62 (1982, CN, W)	91 (1902, NZ, W)	189 (1982, CN, W)	60 (1994, CN, C)
33rd percentile	221	236	387	210
Median	244	288	456	245
Average	253	288	445	247
66th percentile	291	334	516	283
Maximum	440 (1973, CP, N)	548 (1973, CP, N)	709 (1992, CN, W)	500 (1974, RR, C)
CV (%)	32	31	30	33

Table 5. Associations of simulated wheat yields and spring rainfall, with corresponding SOI phase in June–July and Pacific Ocean SSTs events in July for four regions across south-eastern Australia

The contingency table presents tercile values. The numbers in parenthesis are the percentage of years in each tercile for each SOI phase and SST phase (Table 3). (CN: consistently negative; CP: consistently positive; RF: rapidly falling; RR: rapidly rising and NZ: consistently near zero). The χ^2 test value is shown at the bottom of the table. 'df' indicates degrees of freedom and P is the probability of rejecting the null hypothesis (i.e. no association)

SOI phase	Tercile				SST phase	Tercile			
	Lower	Middle	Upper	Total		Lower	Middle	Upper	Total
				Birchip					
Spring rainfall									
CN	8 (53%)	5 (33%)	2 (13%)	15	Cold	8 (21%)	13 (34%)	17 (45%)	38
CP	5 (20%)	6 (24%)	14 (56%)	25	Neutral	9 (25%)	13 (36%)	14 (39%)	36
RF	4 (50%)	3 (38%)	1 (13%)	8	Warm	17 (57%)	10 (33%)	3 (10%)	30
RR	6 (25%)	9 (38%)	9 (38%)	24	Total	34	36	34	104
NZ	11 (34%)	13 (41%)	8 (25%)	32		$\chi^2 = 14.37$; df = 4; $P = 0.006$			
Total	34	36	34	104					
	$\chi^2 = 23.97$; df = 8; $P = 0.002$								
Yield									
CN	8 (53%)	3 (20%)	4 (27%)	15	Cold	7 (18%)	16 (42%)	15 (39%)	38
CP	7 (28%)	10 (40%)	8 (32%)	25	Neutral	15 (42%)	13 (36%)	8 (22%)	36
RF	4 (50%)	1 (13%)	3 (38%)	8	Warm	12 (40%)	7 (23%)	11 (37%)	30
RR	3 (13%)	10 (42%)	11 (46%)	24	Total	34	36	34	104
NZ	12 (38%)	12 (38%)	8 (25%)	32		$\chi^2 = 7.37$; df = 4; $P = 0.117$			
Total	34	36	34	104					
	$\chi^2 = 23.90$; df = 8; $P = 0.002$								
				Dooen					
Spring rainfall									
CN	9 (60%)	3 (20%)	3 (20%)	15	Cold	7 (18%)	18 (47%)	13 (34%)	38
CP	6 (24%)	8 (32%)	11 (44%)	25	Neutral	8 (22%)	13 (36%)	15 (42%)	36
RF	3 (38%)	4 (50%)	1 (13%)	8	Warm	19 (63%)	5 (17%)	6 (20%)	30
RR	4 (17%)	10 (42%)	10 (42%)	24	Total	34	36	34	104
NZ	12 (38%)	11 (34%)	9 (28%)	32		$\chi^2 = 19.18$; df = 4; $P < 0.001$			
Total	34	36	34	104					
	$\chi^2 = 11.54$; df = 8; $P = 0.173$								
Yield									
CN	7 (47%)	1 (7%)	7 (47%)	15	Cold	10 (26%)	14 (37%)	14 (37%)	38
CP	5 (20%)	12 (48%)	8 (32%)	25	Neutral	11 (31%)	14 (39%)	11 (31%)	36
RF	4 (50%)	3 (38%)	1 (13%)	8	Warm	14 (47%)	7 (23%)	9 (30%)	30
RR	5 (21%)	6 (25%)	13 (54%)	24	Total	35	35	34	104
NZ	13 (41%)	14 (44%)	5 (16%)	32		$\chi^2 = 3.89$; df = 4; $P = 0.420$			
Total	34	36	34	104					
	$\chi^2 = 18.75$; df = 8; $P = 0.016$								
				Albury					
Spring rainfall									
CN	11 (73%)	2 (13%)	2 (13%)	15	Cold	10 (26%)	12 (32%)	16 (42%)	38
CP	4 (16%)	8 (32%)	13 (52%)	25	Neutral	8 (22%)	18 (50%)	10 (28%)	36
RF	3 (38%)	3 (38%)	2 (25%)	8	Warm	16 (53%)	6 (20%)	8 (27%)	30
RR	3 (13%)	10 (42%)	11 (46%)	24	Total	34	36	34	104
NZ	13 (41%)	13 (41%)	6 (19%)	32		$\chi^2 = 11.63$; df = 4; $P = 0.020$			
Total	34	36	34	104					
	$\chi^2 = 23.97$; df = 8; $P = 0.002$								
Yield									
CN	12 (80%)	1 (7%)	2 (13%)	15	Cold	9 (24%)	13 (34%)	16 (42%)	38
CP	3 (12%)	13 (52%)	9 (36%)	25	Neutral	10 (28%)	12 (33%)	14 (39%)	36
RF	4 (50%)	2 (25%)	2 (25%)	8	Warm	15 (50%)	11 (37%)	4 (13%)	30
RR	5 (21%)	10 (42%)	9 (38%)	24	Total	34	36	34	104
NZ	10 (31%)	10 (31%)	12 (38%)	32		$\chi^2 = 8.91$; df = 4; $P = 0.064$			
Total	34	36	34	104					
	$\chi^2 = 23.90$; df = 8; $P = 0.002$								
				Griffith					
Spring rainfall									
CN	9 (60%)	4 (27%)	2 (13%)	15	Cold	9 (24%)	10 (26%)	19 (50%)	38
CP	6 (24%)	6 (24%)	13 (52%)	25	Neutral	13 (36%)	12 (33%)	11 (31%)	36

(*continued next page*)

Table 5. (*continued*)

SOI phase	Tercile				SST phase	Tercile			
	Lower	Middle	Upper	Total		Lower	Middle	Upper	Total
RF	4 (50%)	2 (25%)	2 (25%)	8	Warm	12 (40%)	12 (40%)	6 (20%)	30
RR	4 (17%)	8 (33%)	12 (50%)	24	Total	34	34	36	104
NZ	11 (34%)	14 (44%)	7 (22%)	32		$\chi^2 = 7.15$; df = 4; $P = 0.128$			
Total	34	34	36	104					
	$\chi^2 = 16.24$; df = 8; $P = 0.039$								
Yield									
CN	8 (53%)	4 (27%)	3 (20%)	15	Cold	11 (29%)	8 (21%)	19 (50%)	38
CP	4 (16%)	8 (32%)	13 (52%)	25	Neutral	12 (33%)	16 (44%)	8 (22%)	36
RF	3 (38%)	4 (50%)	1 (13%)	8	Warm	11 (37%)	12 (40%)	7 (23%)	30
RR	5 (21%)	9 (38%)	10 (42%)	24	Total	34	36	34	104
NZ	14 (44%)	11 (34%)	7 (22%)	32		$\chi^2 = 9.08$; df = 4; $P = 0.059$			
Total	34	36	34	104					
	$\chi^2 = 13.62$; df = 8; $P = 0.092$								

were used to explore the effect of climate variability and quality of the climate forecasts.

Associations of spring rainfall and wheat yield with the forecasting systems

There were strong and consistent associations of spring rainfall and simulated yield with the climate phases. Table 5 shows changes in the proportison of years within each of the terciles for each of the phases of the forecasting system for spring rainfall and simulated wheat yields. For example, there were 24 rapidly rising SOI (RR) events in the last 104 years. Assuming no association with the SOI 5-phase system, there should be ~8 years in each tercile. However, for Birchip there are 9 and 11 years in the upper tercile for spring rainfall and grain yield, respectively (Table 5), i.e. a higher proportion of spring rainfall (38%) and simulated wheat yield (46%) values in the upper tercile than what would be expected from chance alone (33%). Correspondingly, there are only 6 and 3 RR years in the lower terciles for spring rainfall (25%) and grain yield (13%), respectively. During consistently negative years at the end of July (CN), the opposite pattern was observed. Given the 15 CN events on record, one would again expect ~5 years in each tercile. However, for spring rainfall there were 8 years in the lower tercile (53%) and only 2 (13%) in the upper tercile. For simulated grain yield there were 8 years in the lower tercile (53%) and only 4 (27%) in the upper tercile. The χ^2 *P*-value ($P = 0.002$ for both spring rainfall and wheat yield) indicates that counts in the table cells were significantly different from those expected if spring rainfall and yield were independent of the SOI phases. This level of significance prevailed for spring rainfall and simulated wheat yield across most of the locations studied (Table 5). In regards to the Pacific Ocean SST in July (Table 5), only spring rainfall showed a distinct association with the corresponding Cold, Neutral, and Warm SST phases. The association of simulated wheat yields with Pacific Ocean SST in July appeared to be site dependent, as simulated wheat yields in Wagga Wagga (data not shown) showed a significant χ^2 *P*-value ($P = 0.020$). These results indicated that stronger ENSO signals on spring rainfall and simulated grain yields can be obtained from the SOI 5-phase system, even when the number of phases in this system is higher than in the SST system, i.e. fewer degrees of freedom.

Reliability of the forecasts of spring rainfall and wheat yield

Figure 4 shows the reliability plots for the forecasts of spring rainfall using the June–July SOI phases (Fig. 4*a–d*) and Pacific Ocean SSTs events in July (Fig. 4*e–h*). Accept at Albury (New South Wales) under the SOI 5-phase forecasting system (Fig. 4*c*), probabilities for spring rainfall in the 0–20% forecast category (i.e. 0–20% chance of exceeding the median) and for all four locations in the 80–100% forecast category (i.e. 80–100% chance of exceeding the median) were never forecast. With the exception of Griffith (NSW), and for the Pacific Ocean SSTs events in July (Fig. 4*h*), there was a high number of years in the 20–80% forecast category, with good reliability for the forecast of spring rainfall. For the 40–60% forecast category, the agreement between ORF and *f* was highest under the Pacific Ocean SSTs events at Griffith (74 years) (Fig. 4*h*), Dooen (72 years, under the SOI 5-phase forecasting system) (Fig. 4*b*), and Birchip (69 years, under the SOI 5-phase forecasting system) (Fig. 4*a*). The reliability of the forecast for spring rainfall at Birchip, Dooen, and Griffith was classified as 'Good', with regression slopes of 0.877–1.011 and RMSD values of 0.021–0.077, both under the SOI 5-phase forecasting system and the Pacific Ocean SSTs events. However, at Albury (Fig. 4*c*), even when the reliability for spring rainfall was classified as 'Good', the RMSD value was high (0.397) under the SOI 5-phase forecasting system. These results indicate that the reliability of the forecasts for spring rainfall is site dependent, and that both forecasting systems lack capacity to forecast the extremely good, i.e. above decile 8, and extremely poor seasons, i.e. below decile 2.

Figure 5 shows the reliability plots for the forecasts of simulated wheat yields using the June–July SOI phases (Fig. 5*a–d*) and Pacific Ocean SSTs events in July (Fig. 5*e–h*). The reliability of the SOI 5-phase system to forecast wheat yields was classified as 'Good' for Birchip, Dooen, and Griffith, with regression slopes of 0.772–1.023 (Fig. 5*a*, *b*, *d*). For these locations, the RMSD was 0.063–0.105. Wheat yields were never forecast for the 0–20% range forecast category at Birchip and Griffith (Fig. 5*a*, *d*), but there was a high number of years in the 20% to 80% forecast category for all four locations. For the 40–60% forecast category, the agreement between ORF and *f*

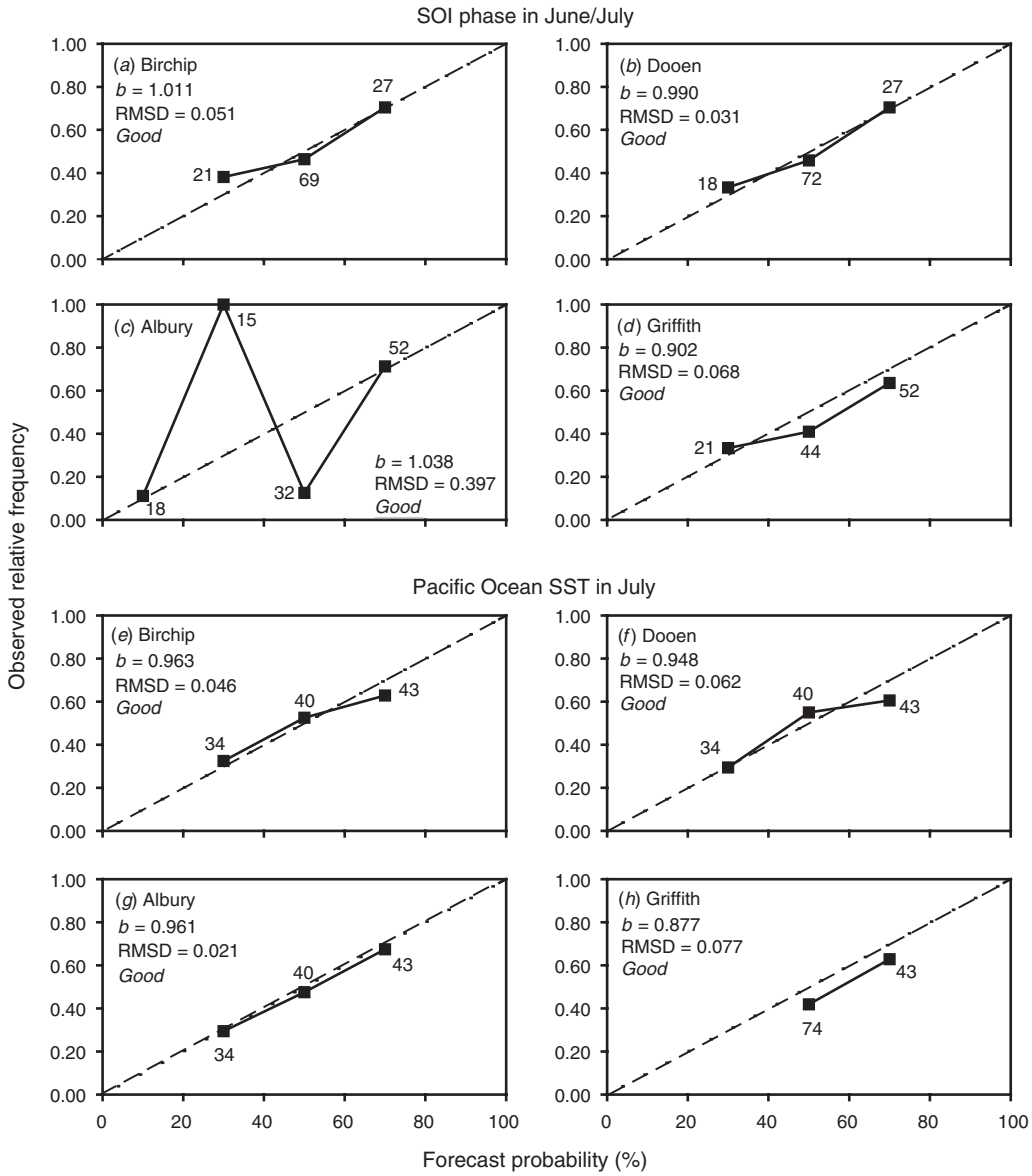

Fig. 4. Reliability diagrams for the probabilistic spring rainfall forecasts at 4 regions across south-eastern Australia for (*a–d*) the SOI phase in June–July, and (*e–h*) the Pacific Ocean SSTs events in July. The filled rectangles represent the data points for observed relative frequency against forecast probability with the numbers of times forecast issued in each forecast probability category. The dashed black line represents the 1 : 1 line of perfect reliability and the solid black line joins the observed relative frequency values at each quintile.

was highest at Griffith (72 years) (Fig. 5*d*), Birchip (65 years) (Fig. 5*a*), Albury (61 years) (Fig. 5*c*) and Dooen (52 years) (Fig. 5*b*). At Birchip and Griffith, the relative error was less than 10%, and for Dooen it was 11%, indicating high reliability of the forecast. The reliability of the forecast for simulated wheat yield at Albury was classified as 'Moderate', with a regression slope of 0.732 (Fig. 5*c*), and a relative error of 20%. In the other locations, the forecasting system was reliable, indicating that the SOI phase system could be used to forecast wheat yields by the end of July. Similarly, at all four locations, the reliability of the Pacific Ocean SST 3-phase system to forecast simulated wheat yields was classified as 'Good', with regression slopes of 0.778–0.995 (Fig. 5*e–h*) and RMSD of 0.063–0.409. From these results, it can be summarised that both SOI and SST phases at the end of July could be used with confidence to forecast wheat yields. However, the forecasts were never issued for the higher and lower deciles, indicating lack of capacity to forecast the extremely good, i.e. above decile 8, and extremely poor seasons, i.e. below decile 2.

Capacity of the June–July SOI phase system and July Pacific Ocean SST phase to discriminate spring rainfall

Significant shifts in median values of spring rainfall were observed between all years and SOI and Pacific Ocean SSTs

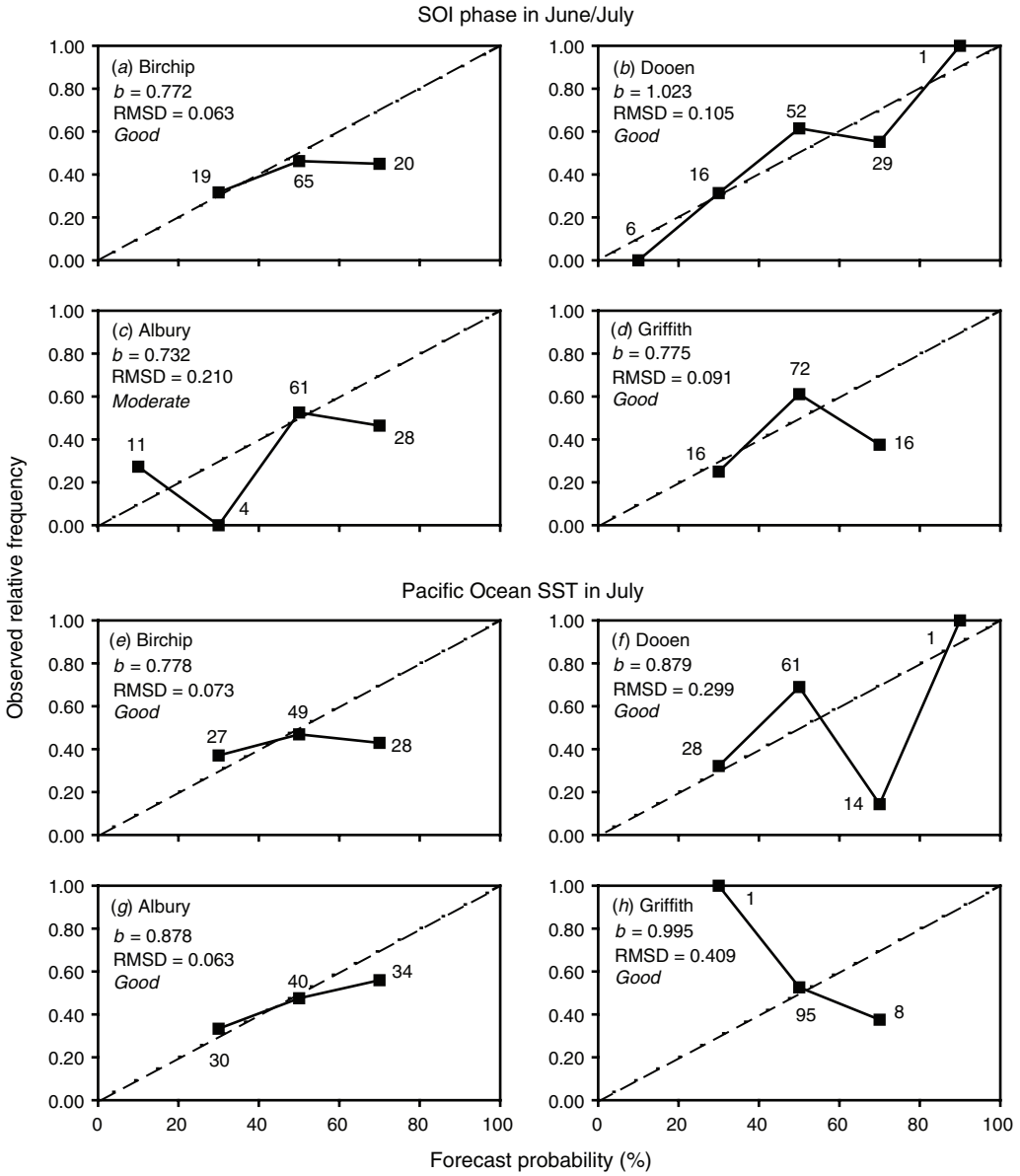

Fig. 5. Reliability diagrams for the probabilistic wheat yield forecasts at 4 regions across south-eastern Australia for (*a–d*) the SOI phase in June–July and (*e–h*) the Pacific Ocean SSTs events in July. The filled rectangles represent the data points for observed relative frequency against forecast probability with the numbers of times forecast issued in each forecast probability category. The dashed black line represents the 1 : 1 line of perfect reliability and the solid black line joins the observed relative frequency values at each quintile.

phases (Fig. 6). Significant ($P < 0.001$) differences in the median values of spring rainfall for the different SOI 5 phases were detected using a KW test (Kruskal and Wallis 1952). The consistently negative (CN) and rapidly falling (RF) SOI phases during June–July, and Warm events of Pacific Ocean SSTs in July indicated a greater likelihood of lower amounts of spring rainfall across all locations. Consistently positive (CP) and rapidly rising (RR) SOI phases in June–July, and Cold events in the Pacific Ocean in July, indicated greater chance of higher spring rainfall. Additionally, different SOI phases in June–July and Pacific Ocean SST events in July had contrasting discrimination capacities (KS tests; Conover 1971). Across all locations, the SOI phases, except RR at Birchip, were able to significantly discriminate shifts in median values of spring rainfall. The Pacific Ocean SST phases (Fig. 6) also significantly discriminated spring rainfall.

Changes in the medians and in the dispersion of the probability distribution functions were also evaluated by calculating the values of the absolute median difference (AMD) and the inter-quartile ratio (IQR), for both the SOI 5 phases, and the Pacific Ocean SSTs (Fig. 6). In general, AMD was higher for the CP and RR phases than for the CN and RF phases (Fig. 6). There were no consistent effects on the values of IQR, except for the CN phase, i.e. lower variability at all locations. From these

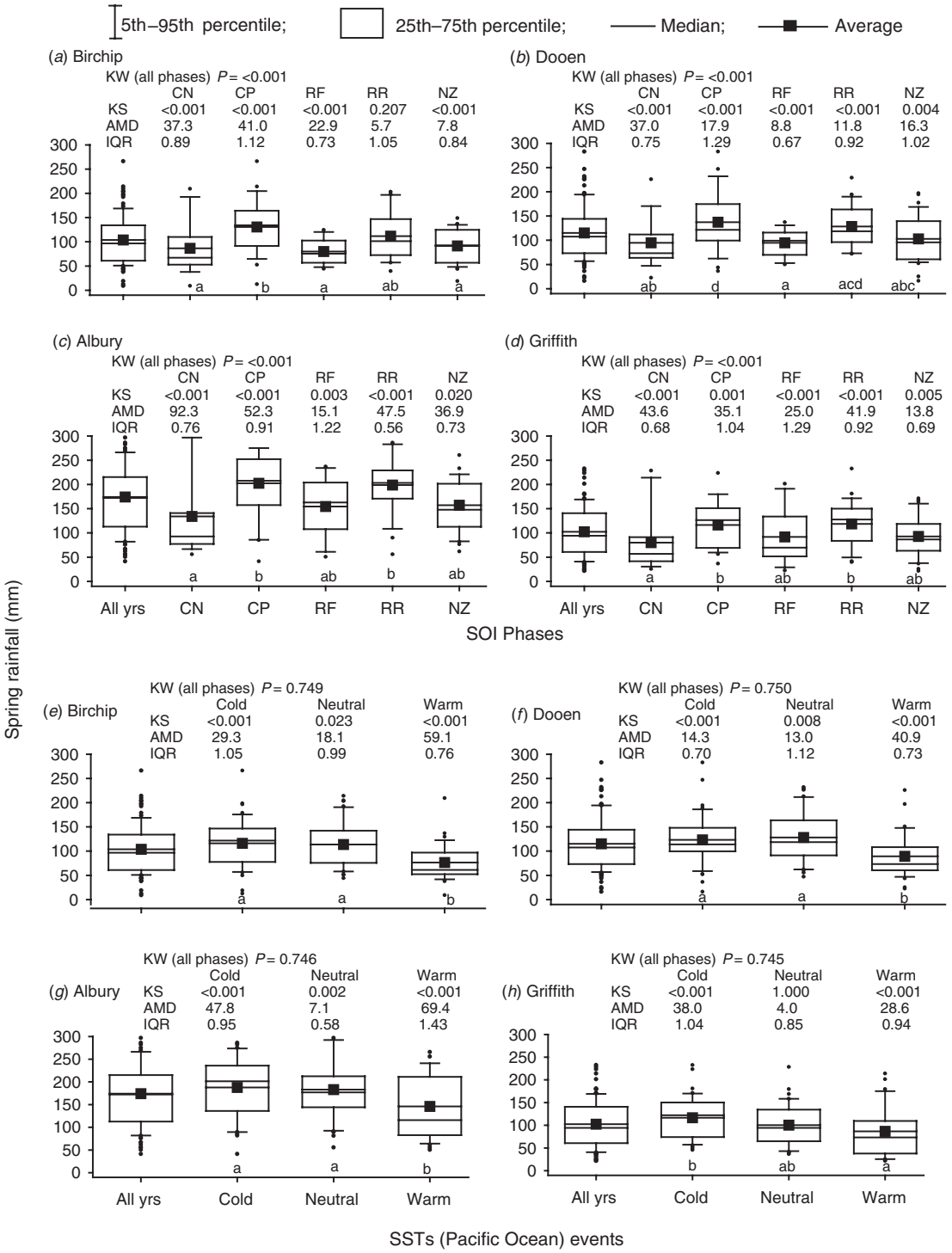

Fig. 6. Relative frequency (%) distribution of spring rainfall at 4 regions across south-eastern Australia for each (*a–d*) SOI phase in June–July and (*e–h*) the Pacific Ocean SSTs events in July. Means of ENSO phases with common letters below their respective box-and-whiskers are not significantly different ($P \leq 0.05$). The significance of the shift in the medians in each phase away from the All-years value was measured using the Kruskal-Wallis test (KW) and the similarity of distributions by the Kolmogorov–Smirnov *P*-value test (KS). The shift is measured using the absolute median difference (AMD), while changes in the distribution dispersion are measured using the inter-quartile ratio (IQR). All yrs, Actual years used, i.e. 1900–2003; CN, consistently negative; CP, consistently positive; RF, rapidly falling; RR, rapidly rising; NZ, consistently near zero.

results, it can be summarised that different SOI and SST phases at the end of July had contrasting capacities to discriminate for changes in spring rainfall.

Wheat yield analysis based on June–July SOI phase system and Pacific Ocean SST phase in July

Figure 7 shows important shifts in the median values of the cumulative probability distribution function for simulated wheat yields. During CN and RF phases in June–July, the probability distribution function shifts towards lower yields at almost all the locations. Median grain yields are reduced by ~20–43%, 4–32%, 9–56%, and 7–77% for CN and RF SOI phases in Birchip, Dooen, Albury, and Griffith, respectively (Fig. 7*a–d*), compared with the rest of the years. In contrast, during the CP SOI phase, the probability distribution function shifts towards higher median wheat yields at all locations (Fig. 7). Cumulative probabilities for the simulated wheat yields under the Pacific Ocean SST phase in July (Fig. 7*e–h*), also showed considerable shifts in the median values among cold, neutral, and warm events. Median yield values were higher during cold events, than during warm events, with neutral years falling in between. Shifts in median values among all SOI and SST phases were highly significant ($P < 0.001$) (Fig. 7).

Changes in the medians and in the dispersion of the probability distribution functions were evaluated by calculating the absolute median difference (AMD), and the inter-quartile ratio (IQR) (Fig. 7). At Birchip (Fig. 7*a*), higher yields, i.e. AMD = 126 kg/ha and 277 kg/ha, and reduced variability, i.e. IQR = 0.72 and 0.52, could be expected under CP or RR SOI phases in July, respectively. Similarly, lower yields, i.e. AMD = 313 kg/ha and 583 kg/ha, and increased variability, i.e. IQR = 1.64 and 2.6, could be expected during RF and CN phases in July, respectively.

Forecasts consistency

Cross-validation techniques were used to evaluate the skill of the SOI 5-, and Pacific Ocean SST 3-phase forecasting systems (Figs 8, 9). This method quantifies the number of times (as a percentage) that the probability swing, i.e. for above and below long-term median, was in the direction subsequently observed. In general, the overall skill of the SOI phase system was slightly higher than that for the Pacific Ocean SSTs system. As an example, we present and discuss the results for spring rainfall (Fig. 8*a*) and simulated grain yield (Fig. 9*a*) at Birchip. The overall skill of the SOI system, i.e. % consistent, for spring rainfall (Fig. 8*a*) at the end of July was 61%. The values of % consistent were highest for the consistently positive (76%) and consistently negative (73%) phases. The overall skill of the Pacific Ocean SSTs system for spring rainfall was 70%. The consistency of the system was highest for the warm (90%) and cold (68%) events.

The overall skill of the SOI system for simulated yields at Birchip (Fig. 9*a*) was 60% consistent. The values of % consistent were highest during the rapidly rising (80%) and consistently negative (67%) phases. Values of % consistent lower than 50% indicate the absence of forecast skill. The overall skill of the Pacific Ocean SSTs for simulated wheat yields at Birchip was 59% consistent. The highest consistency was observed for the cold events (66%), while for the warm events it was 57%. Similar forecasting capacity and important variations in the predictive consistency for the different phases of the SOI and SST were observed across the other locations (Figs 8, 9).

Discussion

Our results confirm that ENSO has important effects on the existing variability (Figs 6, 7) in spring rainfall and simulated wheat yields in south-eastern Australia. Both forecasting systems tested here, i.e. the 5-phase SOI (Stone *et al*. 1996) and the 3-phase Pacific Ocean SST (Drosdowsky 2002) systems, can be used with the help of crop models, to translate general, i.e. climate datasets, into value-added targeted, i.e. crop yields, information for decision makers (Hammer *et al*. 1996). The additional value of targetted information resides in the fact that crop yields are not only affected by rainfall, but by several climatic, edaphic, and biological processes that crop simulation models are able to account for (Rodriguez and Sadras 2007).

The close association between spring rainfall, or simulated wheat yields and both the June–July SOI phase, and July Pacific Ocean SST phase systems (Table 5), would allow wheat and canola growers to consider more flexible nitrogen top-dressing practices (Lythgoe *et al*. 2004), and to take full advantage of existing seasonal climate risk management tools. Spring rainfall showed a clear association with the Pacific Ocean SST in July (Table 5), across most of the studied locations, i.e. during a cold (warm) event there is an increased likelihood of higher (lower) than normal rainfall during August–October. In south-eastern Australia the August–October period coincides with the critical stages for grain yield definition in wheat (Rodriguez and Sadras 2007). For wheat and canola, wet and mild conditions during early spring are usually associated with high yielding seasons (Fischer 1979; McCallum *et al*. 2000), seasons during which farmers would certainly profit from turning up crop nitrogen nutrition.

A variety of forecast verification procedures exists which involve measures of the relationship between a forecast and the corresponding observation of a predictand (Wilks 1995). In this work we have assessed the quality of the SOI and SST phase systems by studying four attributes of their performance: their reliability, accuracy, and the relative degree of shift and dispersion of the distributions (Wilks 1995; Potgieter *et al*. 2003).

The analysis of reliability in Figs 4 and 5 indicated that in SEA, both the SOI phase system and the Pacific Ocean SST 3-phase system can be used with confidence to forecast spring rainfall or wheat yield as early as the end of July. However, they also indicate their lack of capacity to identify the most critical extremely good and extremel poor seasons, in which farmers make most, or lose most of their financial capital.

At all four locations, with both the June–July SOI phases and the Pacific Ocean SSTs events in July, the agreement between ORF and f was highest for the 40–60% forecast category. With the exception of Albury (Fig. 5*c*), which had only moderate reliability ($b = 0.732$, RMSD = 0.21) of forecast wheat yields using the SOI 5-phase system, the reliability of the forecasting system was greatest for spring rainfall (Fig. 5), with small values

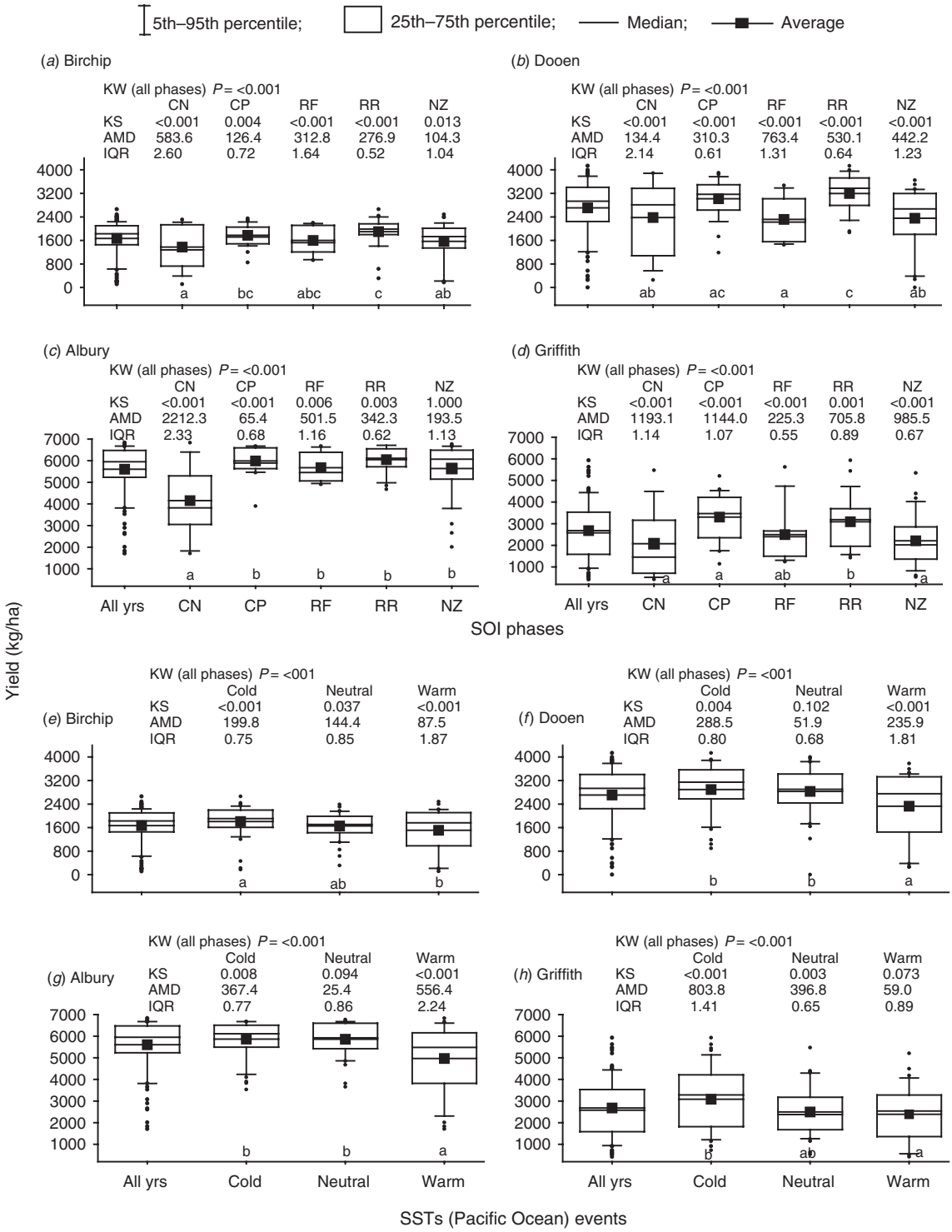

Fig. 7. Relative frequency (%) distribution of simulated wheat yields at 4 regions across south-eastern Australia for each (*a–d*) SOI phase in June–July and (*e–h*) the Pacific Ocean SSTs events in July. Specific soil and management conditions have been used in the analyses (see text). Means of ENSO phases with common letters below their respective box-and-whiskers are not significantly different ($P \leq 0.05$). The significance of the shift in the medians in each phase away from the All-years value was measured using Kruskal-Wallis test (KW) and the similarity of distributions by the Kolmogorov-Smirnov *P*-value test (KS). The shift is measured using the absolute median difference (AMD), while changes in the distribution dispersion are measured using the inter-quartile ratio (IQR). All years and phases as in Fig. 5.

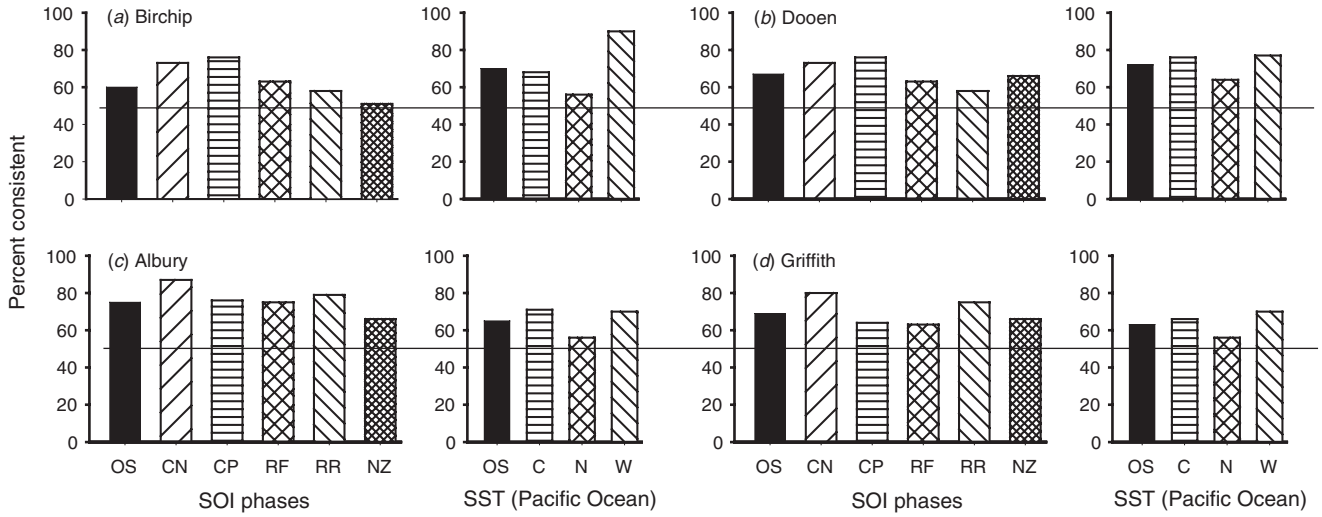

Fig. 8. The predictive consistency of spring rainfall forecasts at the end of July by cross-validation of % consistent based on SOI and SST phase forecast systems in 4 regions across south-eastern Australia: (*a*) Birchip and (*b*) Dooen in Victoria; (*c*) Albury and (*d*) Griffith in New South Wales. OS, Overall skill; CN, consistently negative; CP, consistently positive; RF, rapidly falling; RR, rapidly rising; NZ, consistently near zero; C, Cold Pacific; N, Neutral Pacific; W, Warm Pacific. Horizontal line at 50% consistent.

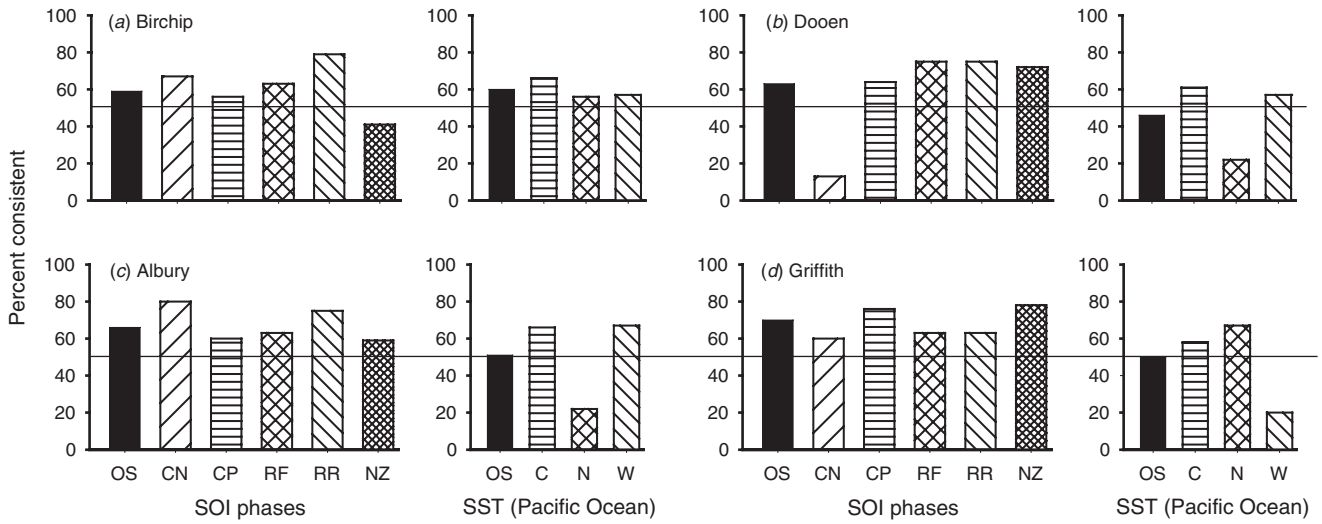

Fig. 9. The predictive consistency of simulated wheat yield forecasts at the end of July via cross-validation of % consistent based on SOI and SST phase forecast systems in 4 regions across south-eastern Australia: (*a*) Birchip and (*b*) Dooen in Victoria; (*c*) Albury and (*d*) Griffith in New South Wales. OS, Overall skill; CN, consistently negative; CP, consistently positive; RF, rapidly falling; RR, rapidly rising; NZ, consistently near zero; C, Cold Pacific; N, Neutral Pacific, W, Warm Pacific. Horizontal line at 50% consistent.

of RMSD in most of the locations across SEA. The moderate reliability of the forecast wheat yield at Albury indicated that forecasts of wheat yield made by the end of July would be better made using the SST system. Further, the higher reliability of spring rainfall forecast than wheat yield could be related to the fact that the predictability of crop yields is subject to the accumulation of the errors in predicting yields from seasonal rainfall (Hansen *et al*. 2004).

Significant shifts in median values for both spring rainfall and simulated wheat yields were observed from applying both forecasting systems (Figs 6, 7). Our results confirm those of Hammer *et al*. (1996) and Potgieter *et al*. (2002), that a substantial portion of the inter-annual variability in simulated wheat yield is associated with ENSO-related variability. Shifts in median values of spring rainfall based on the June–July SOI phase (Fig. 6*a–d*) indicate some discrimination capacity for this variable at all locations across SEA. The KW test (Kruskal and Wallis 1952) for the July Pacific Ocean SST phases showed no significant differences in median values of spring rainfall (Fig. 6*e–h*). However, significant differences according to a KS non-parametric test (Conover 1971) were observed in cumulative distributions of spring rainfall, which indicates that high (low) spring rainfall is more frequent during cold (warm) events.

Significant shifts in median values of simulated grain yield based on the June–July SOI phases and Pacific Ocean SSTs events in July (Fig. 7) were also observed. For example, at Albury (Fig. 7*c*), the median simulated yield during consistently negative SOI years in June–July, was 3816 kg/ha, which is about 30–37% lower than the median yield for either the rest of the years or the other four SOI phases. The impact of ENSO on wheat production in SEA differs among locations and months of the year (Rodriguez and Luo 2003).

In addition to changes in the median values (AMD), changes in dispersion (IQR), for spring rainfall and simulated wheat yields were also associated with ENSO. The inter-quartile ratio (Figs 6*d*, 7*d*) during a CP SOI phase at Griffith was close to 1 for both spring rainfall (1.04) and simulated wheat yield (1.07), indicating that during CP phases, simulated wheat yields would fluctuate less around the long-term median. Therefore, during those years with CP SOI phase changing crop management, e.g. top-dressing nitrogen fertilisers, could produce economic benefits (Hammer *et al*. 1996; Lythgoe *et al*. 2004; Hayman 2006).

The consistency of both forecasting systems was relatively constant across the regions and tended to be higher for spring rainfall than for simulated grain yields. The overall skill of the SOI 5-phase system for spring rainfall and simulated wheat yields at the end of July varied from 60 to 78% consistent. The overall skill of the Pacific Ocean SST phase system ranged from no skill at all to 72% consistent in Victoria. This would indicate that there might be potential for farmers to benefit from the adoption of more flexible management approaches to take full advantage of the climate information. When skill of the forecasting system was dissected on the performance of each individual phase, a consistent pattern emerged. Different phases of the SOI and the SST showed different contribution to the overall predictive consistency of the forecasts. In general terms the consistently positive and consistently negative phases, as well as the cold and warm events, seemed to have a stronger signal than the others. However, this was highly location dependent. At this stage it is unclear, however, if these regional contrasts are robust or merely the result of sampling variance. Consequently, some phases might be more useful than others, although this warrants further investigation.

Conclusions

We observed significant ENSO signals as early as the end of July, on the spring rainfall and expected grain yields in south-eastern Australia (SEA), which can be used to help growers make better decisions. Spring rainfall and simulated wheat yields showed associations with the studied forecasting systems. Whether this would allow farmers to make better tactical nitrogen applications needs to be better evaluated. We observed significant changes in the probability distribution functions of grain yield and spring rainfall, when using either the SOI or SST phase systems in June–July. Changes in shift and dispersion can be useful to inform better tactical farming management options. Our analysis of reliability and forecast consistency indicated that the forecasts can be used to make potentially useful seasonal outlooks for grain yield. The overall predictive skill for spring rainfall and simulated wheat yield ranged from 60 to 83% consistent. The consistency was site specific and different phases of the SOI and SST made different contributions to the overall predictive level of both forecasting systems.

Acknowledgments

The authors thank Andries Potgieter at the Queensland Department of Primary Industries and Fisheries for his valuable comments on methodology for reliability analysis. This study was supported by PIRVic and the Grains Research and Development Corporation through grant DAV00006. We thank Drs Kim Lowell, Helen Fairweather, and an anonymous referee for helpful comments on an early version of the manuscript.

References

Angus JF (2001) Nitrogen supply and demand in Australian agriculture. *Australian Journal of Experimental Agriculture* **41**, 277–288. doi: 10.1071/EA00141

Asseng S, Fillery IRP, Anderson GC, Dolling PJ, Dunin FX, Keating BA (1998) Use of the APSIM wheat model to predict yield, drainage, and NO_3^- leaching for a deep sand. *Australian Journal of Agricultural Research* **49**, 363–377. doi: 10.1071/A97095

Conover WJ (1971) 'Practical nonparametric statistics.' (John Weley & Sons, Inc.: New York)

Dalgliesh N, Foale M (1998) 'Soil matters, monitoring soil water and nutrients in dryland farming.' (Agricultural Production Systems Research Unit: Toowoomba, Qld)

Drosdowsky W (2002) SST phases and Australian rainfall. *Australian Meteorological Magazine* **51**, 1–12.

Fischer RA (1979) Growth and water limitation to dryland wheat yield in Australia: a physiological framework. *Journal of the Australian Institute of Agricultural Science* **45**, 83–94.

Hammer GL (2000) A general systems approach to applying seasonal climate forecasts. In 'Applications of seasonal climate forecasting in agricultural and natural ecosystems – the Australian experience'. (Eds GL Hammer, N Nicholls, C Mitchell) pp. 51–65. (Kluwer Academic: Dordrecht, The Netherlands)

Hammer GL, Holzworth DP, Stone R (1996) The value of skill in seasonal climate forecasting to wheat crop management in a region with climatic variability. *Australian Journal of Agricultural Research* **47**, 717–737. doi: 10.1071/AR9960717

Hansen JW, Potgieter A, Trippet MK (2004) Using a general circulation model to forecast regional wheat yields in northeast Australia. *Agricultural and Forest Meteorology* **127**, 77–92. doi: 10.1016/j.agrformet.2004.07.005

Hayman P (2006) Communicating skilful but uncertain seasonal climate forecasts. In 'Proceedings of the workshop on the science of seasonal climate prediction'. The Shine Dome, Canberra, ACT, 2–3 August 2006. Available at: www.science.org.au/events/seasonal/index.htm

Hayman P, Fawcett R (2004) CAVP project report 'Seasonal climate forecasting and the south eastern grains belt'. Available at: www.cvap.gov.au/newfsG3publications.html

Keating BA, Carberry PS, Hammer GL, Probert ME, Robertson MJ, *et al*. (2003) An overview of APSIM, a model designed for farming systems simulation. *European Journal of Agronomy* **18**, 267–288. doi: 10.1016/S1161-0301(02)00108-9

Kruskal WH, Wallis WA (1952) Use of ranks on one-criterion variance analysis. *Journal of the American Statistical Association* **48**, 907–911. doi: 10.2307/2281082

Lythgoe B, Rodriguez D, De Li Liu, Brennan J, Scott B, Murry G, Hayman P (2004) Seasonal climate forecasting has economic value for farmers in south eastern Australia. In 'Proceedings of the 4th International Crop Science Congress'. Brisbane, Qld, 26 Sep.–1 Oct. 2004, p. 204. ISBN 1 920842 20 9. Available at: www.cropscience.org.au/icsc2004/poster/2/6/524_rodriguezd.htm

McCallum MH, Peoples MB, Connor DJ (2000) Contributions of nitrogen by field pea (*Pisum sativum* L.) in a continuous cropping sequence compared with a lucerne (*Medicago sativa* L.)-based pasture ley in the Victorian Wimmera. *Australian Journal of Agricultural Research* **51**, 13–22. doi: 10.1071/AR99023

McCown RL, Hammer GL, Hargreaves JNG, Holzworth DP, Freebairn DM (1996) APSIM: a novel software system for model development, model testing, and simulation in agricultural systems research. *Agricultural Systems* **50**, 255–271. doi: 10.1016/0308-521X(94)00055-V

Meinke H, Hochman Z (2000) Using seasonal climate forecasts to manage dryland crops in northern Australia. In 'Applications of seasonal climate forecasting in agricultural and natural ecosystems – the Australian experience'. (Eds GL Hammer, N Nicholls, C Mitchell) pp. 149–165. (Kluwer Academic: Dordrecht, The Netherlands)

Meinke H, Stone RC, Hammer GL (1996) SOI phases and climatic risk to peanut production: a case study for northern Australia. *International Journal of Climatology* **16**, 783–789. doi: 10.1002/(SICI)1097-0088(199607)16:7<783::AID-JOC58>3.0.CO;2-D

Murphy AH, Winkler RL (1992) Diagnostic verification of probability forecasts. *International Journal of Forecasting* **7**, 435–455. doi: 10.1016/0169-2070(92)90028-8

Nuttall JG, Armstrong RD, Connor DJ (2003) Evaluating physicochemical constraints of Calcarosols on wheat yield in the Victorian southern Mallee. *Australian Journal of Agricultural Research* **54**, 487–497. doi: 10.1071/AR02168

Potgieter AB, Everingham YL, Hammer GL (2003) On measuring quality of a probabilistic commodity forecast for a system that incorporates seasonal climate forecasts. *International Journal of Climatology* **23**, 1195–1210. doi: 10.1002/joc.932

Potgieter AB, Hammer GL, Butler D (2002) Spatial and temporal patterns in Australian wheat yield and their relationship with ENSO. *Australian Journal of Agricultural Research* **53**, 77–89. doi: 10.1071/AR01002

Power S, Casey C, Folland C, Mehta V (1999) Inter-decadel modulation of the impact of ENSO on Australia. *Climate Dynamics* **15**, 319–324. doi: 10.1007/s003820050284

Power S, Tseitkin F, Torok S, Lavery B, Dahni R, McAvaney B (1998) Australian temperature, Australian rainfall and the Southern Oscillation, 1910–1992: coherent variability and recent changes. *Australian Meteorological Magazine* **47**, 85–101.

Rimmington GM, Nicholls N (1993) Forecasting wheat yields in Australia with the Southern Oscillation Index. *Australian Journal of Agricultural Research* **44**, 625–632. doi: 10.1071/AR9930625

Rodriguez D, Luo QJ (2003) Farmer's risk-exposure to climate variability in south eastern Australia. Project report: DAV00006-Tools to reduce the impact of climate variability in south-eastern Australia, DPI-Vida, Landscape Systems. Horsham, Vic.

Rodriguez D, Nuttal J (2003) Adaptation of the APSIM-Wheat module to simulate the growth and production of wheat on hostile soils. In 'Proceedings of the 11th Australian Agronomy Conference'. Geelong, Vic. (Australian Society of Agronomy: Geelong, Vic.)

Rodriguez D, Nuttall J, Sadras VO, van Rees H, Armstrong R (2006) Impact of subsoil constraints on wheat yield and gross margin on fine-textured soils of the southern Victorian Mallee. *Australian Journal of Agricultural Research* **57**, 355–365. doi: 10.1071/AR04133

Rodriguez D, Sadras VO (2007) The limit to wheat water-use efficiency in eastern Australia. I. Gradients in the radiation environment and atmospheric demand. *Australian Journal of Agricultural Research* **58**, 287–302. doi: 10.1071/AR06135

Sadras VO, Baldock J, Roget D, Rodriguez D (2003) Measuring and modelling yield and water budget components of wheat crops in coarse-textured soils with chemical constraints. *Field Crops Research* **84**, 241–260. doi: 10.1016/S0378-4290(03)00093-5

Sadras VO, Roget DK, O'Leary GJ (2002) On-farm assessment of environmental and management constraints to wheat yield and rainfall use efficiency in the Mallee. *Australian Journal of Agricultural Research* **53**, 587–598. doi: 10.1071/AR01150

Stephens DJ, Butler DG, Hammer GL (2000) Using seasonal climate forecasts in forecasting the Australian wheat crop. In 'Applications of seasonal climate forecasting in agricultural and natural ecosystems—the Australian experience'. (Eds GL Hammer, N Nicholls, C Mitchell) pp. 351–366. (Kluwer Academic: The Netherlands)

Stone RC, Auliciems A (1992) SOI phase relationships with rainfall in eastern Australia. *International Journal of Climatology* **12**, 625–636. doi: 10.1002/joc.3370120608

Stone RC, Hammer GL, Marcussen T (1996) Prediction of global rainfall probabilities using phases of the Southern Oscillation Index. *Nature* **384**, 252–255. doi: 10.1038/384252a0

Wilks DS (1995) 'Statistical methods in the atmospheric sciences – an introduction.' (Academic Press: London)

Manuscript received 24 April 2007, accepted 10 October 2007